なし

3. その他

なし

厚生労働科学研究費補助金(新型インフルエンザ等新興・再興感染症研究事業)
分担者研究報告書

海外からの侵入が危惧される野生鳥獣媒介性感染症の疫学、診断・予防法等に関する研究

野生鳥獣類媒介性感染症の病理学的検索

—Hantaan ウイルス AA57 株感染マウスの病理学的検討—

分担研究者:永田典代(国立感染症研究所　感染病理部第二室　室長)
協力研究者:佐藤由子(国立感染症研究所　感染病理部　主任研究官)
長谷川秀樹(国立感染症研究所　感染病理部　部長)

研究要旨: Hantaan ウイルス感染症の動物モデル開発を目的として、Hantaan ウイルス実験的感染マウスの病理学的検討を行った。検索対象標本は、代表研究者の苅和らより提供された Hantaan ウイルス AA57 株の皮下接種後の瀕死動物とした。これらの動物の半数では胸水の貯留、肺血管周囲の中等度の水腫、好中球、単核系細胞浸潤を認めた。また、病変部の血管内皮細胞にウイルス抗原陽性細胞が存在した。これらの所見から、ウイルス感染、増殖によって血管内皮細胞が傷害され、肺水腫と胸水貯留が引き起こされたと示唆された。臨床症状と病理所見から、本感染実験系はハンタウイルス肺症候群の動物モデルとして有用であると考えられた。

A. 研究目的

ハンタウイルス感染症には腎症候性出血熱(HFRS, Hemorrhagic fever with renal syndrome)およびハンタウイルス肺症候群(HPS, Hantavirus Pulmonary Syndrome)が知られているが、いずれも動物モデルが確立できておらず、発症機序は不明である。苅和らは極東ロシアのセスジアカネズミ(*Apodemus agrarius*)から分離された Hantaan ウイルスの AA57 株が 2 週齢の ICR マウスに肺疾患を引き起こすことを見いだした。そこで、この感染実験系がハンタウイルス感染症動物モデルとして有用かを評価するために、病理学的検討を行った。

B. 研究方法

2週齢のICRマウスにAA57株を30,000 FFU量皮下接種したところ、接種7-10日目に体重が減少し、呼吸困難となった。これらの発症動物を接種7-11日目に解剖し、病理学的検索対象とした。これらの10%ホルマリン緩衝液固定後のAA57感染マウス組織材料(肺、心、脳、肝、脾、腎)は苅和代表研究者より提供された。常法どおりパラフィン包埋切片を作製した。脱パラフィン後、一部はヘマトキシリン・エオジン(HE)染色を実施した。また、ウイルス抗原を検出するために、一次抗体として抗E5/G6モノクローナル抗体(苅和代表研究者より供与)を用いて免疫組織化学染色を実施した。脱パラフィンした切片を抗原賦活化剤(10mM クエン酸緩衝液　pH6.0)中で121℃　10分オートクレーブ処理によって抗原賦活化した。その後、過酸化水素水・メタノールによる内因性ペルオキシダーゼの阻止を室温30分で処

理し、1次抗体(1μg/ml)を加え4℃で一晩インキュベートした。Vector M.O.M.キットを用いてプロトコール通り免疫染色を実施した。

C. 研究結果

発症動物の解剖を行ったところ、半数の動物が300-400μlの胸水を貯留しており、呼吸困難の原因であることが明らかとなった。病理組織検索の結果、中小の肺血管周囲に軽度の好中球、単核系細胞浸潤を伴う中等度の水腫が認められた(図)。病変部の血管内皮細胞は変性し、好中球の接着が見られた。さらにこの病変に一致してウイルス抗原陽性細胞が存在した。また、肺胞壁には好中球等の細胞浸潤が見られ、軽度の炎症所見が得られた。肺胞内には変化は見られなかった。

D. 考察

全体に炎症性細胞浸潤は軽微で、肺水腫と胸水貯留を引き起こす血管透過性亢進が病変の主体であると考えられた。中小の血管内皮の所見から、血管内皮細胞へのウイルス感染と増殖の結果、細胞が傷害され、肺水腫と胸水貯留の原因となったと考えられた。AA57 株感染後の ICR マウスにおける病変形成は気道系ではなく血管系の肺傷害であることが明らかとなった。発症機序と病態の進行について、今後さらに検討する必要がある。

E. 結論

Hantaan ウイルス AA57 接種後の発症マウスの臨床症状と病理所見から、本実験系は、ハンタウイルス肺症候群の動物モデルとしての有用性が期待される。

F. 健康危険情報

なし。

G. 研究発表

1. 論文発表

1) Seto T, Nagata N, Yoshikawa K, Ichii O, Sanada T, Saasa N, Ozaki Y, Kon Y, Yoshii K, Takashima I, Kariwa H. Infection of Hantaan virus strain AA57 leading to pulmonary disease in laboratory mice. Virus Res. 2012. 163:284-290.

2) Sanada T, Kariwa H, Nagata N, Tanikawa Y, Seto T, Yoshimatsu K, Arikawa J, Yoshii K, Takashima I. Puumala virus infection in Syrian hamsters (Mesocricetus auratus) resembling hantavirus infection in natural rodent hosts. Virus Res. 2011.160:108-119.

2. 学会発表

1) Seto T, Nagata N, Yoshikawa K, Ichii O, Sanada T, Saasa N, Kon Y, Yoshii K, Kariwa H. Development of the lethal animal model of human hantavirus infection. International union of microbiological societies 2011 Congress. Sapporo. Japan. 2011.9

2) Nagata N, Iwata N, Hasegawa H, Sato Y, Morikawa S, Sata T. Interferon gamma protects adult BALB/c mice from lethal respiratory illness after mouse-adapted SARS-CoV infection. International union of microbiological societies 2011 Congress. Sapporo. Japan. 2011.9.

H. 知的財産権の出願、登録状況

なし。

図 AA57株皮下接種後8日目に解剖した2週齢のICRマウスの肺組織像。(左図)わずかな細胞浸潤を伴った、中等度の肺血管周囲の水腫(＊)がみられる。(中央図)血管壁には丸くなった血管内皮、好中球の接着が見られる(矢頭)。(右図)この病変部に一致してウイルス抗原陽性細胞が認められる。

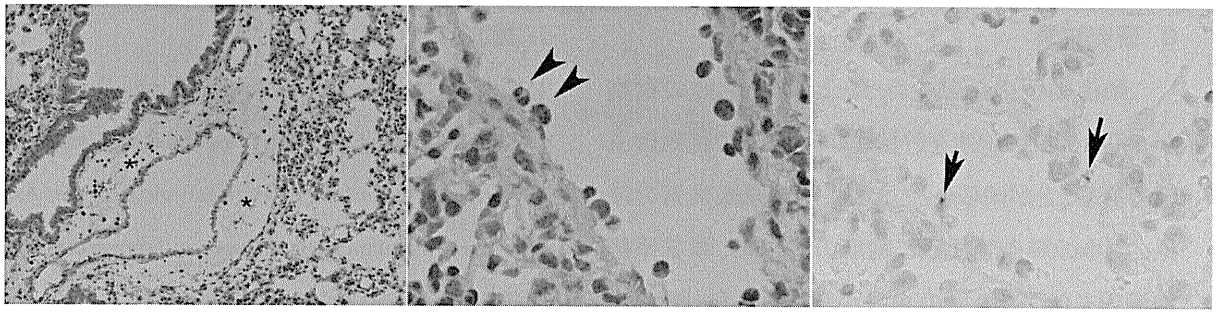

厚生労働科学研究費補助金（新型インフルエンザ等新興・再興感染症研究事業）
分担研究報告書

海外からの侵入が危惧される野生鳥獣媒介性感染症の疫学、診断・予防法等に関する研究
ダニ媒介性脳炎の発症機構の解析および迅速診断法の確立

研究分担者：早坂大輔　長崎大学熱帯医学研究所ウイルス学分野　助教
研究協力者：Mya Myat Ngwe Tun　長崎大学熱帯医学研究所ウイルス学分野　COE 研究員
青木康太郎　長崎大学熱帯医学研究所ウイルス学分野　技能補佐員

研究要旨：ダニ媒介性脳炎（Tick-borne encephalitis, TBE）は、重症化し髄膜炎・脳炎を起こすと致死性が高く、回復しても患者の多くは後遺症が問題となる。しかしながら、重症化に至る機序については不明な点が多く特異的な予防・治療法は確立されていない。そこで本研究では、重症化の要因やリスクファクターのてがかりを探るために、マウスモデルを用いた TBE 発症機序の解析を行った。また、迅速で簡便な TBE 診断法の確立を目指し、Loop-Mediated Isothermal Amplification（LAMP）法による TBEV 遺伝子検出法の検討を行った。その結果、1）IL-10 KO B6 マウスの TBE ウイルス（TBEV）Oshima 株感染では B6 マウスにくらべて重症化の亢進がみられた。しかしながら、中枢神経組織内のウイルス量は IL-10 KO B6 マウスと B6 マウスに顕著な違いがみられなかったことから、重症化には感染個体の免疫応答（免疫病原性）が関わっている可能性が示唆された。2）E 蛋白と NS1 蛋白領域の遺伝子配列を基に LAMP プライマーを設計し、TBEV 全長遺伝子 cDNA を用いて LAMP 解析を行った結果、両領域とも 10^1 コピー以上の TBEV 遺伝子検出が可能であった。

A. 研究目的

TBEV はマダニの吸血によりヒトに感染し、急性の熱性疾患、髄膜炎・脳炎を引き起こす人獣共通感染症の病原体である。我が国においては北海道にロシア春夏脳炎型（極東型）の TBEV 流行巣があることが確認されている。ヒトの TBEV 感染は熱性疾患で済む場合もあるが、髄膜炎・脳炎を起こし重症化すると致死性が高く、回復しても後遺症が残るため、その感染予防や重症化予防が公衆衛生上非常に重要となる。しかしながら、重症化の要因やリスクファクターは十分解明されておらず、特異的な予防・治療法は確立されていない。

我々はマウスモデルを用いたこれまでの研究により、TBEV 感染後の重症個体で IL-10 応答の上昇を示唆してきた。すなわち、B6 マウスに TBEV Oshima 株を皮下感染させると、重症化して死に至る個体（重症個体）と軽症で経過し生き残る個体（軽症個体）がみられるが、重症個体では軽症個体にくらべ脾臓における IL-10

の発現量が上昇していた。そこで、本研究では重症化における IL-10 応答の役割を調べるために、IL-10 KO マウスを用いて病態発現機序の解析を行った。

また、TBEV 感染予防には迅速な診断や流行巣の把握が非常に重要となる。そこで患者血清やマダニから迅速かつ簡便に TBEV 遺伝子を検出できる診断系の確立を目指し、LAMP 法による TBEV 遺伝子検出法の確立を試みた。

B. 研究方法

極東型 TBEV である Oshima 株、Sofjin 株を BHK 細胞で培養後ストックウイルスとした。

1）B6 マウスおよび IL-10 KO B6 マウスに Oshima 株、Sofjin 株をそれぞれ 10^4 PFU 皮下感染させ、体重減少、症状、致死性を比較した。さらに、感染後 5, 9 日目における中枢神経組織中のウイルス量を測定した。また、5, 9 日目における血清中の IgM と IgG 抗体価を ELISA 法にて測定した。統計処理は Gehan-Breslow-Wilcoxon test、Mann-Whitney test により検定した。

2）LAMP プライマー作製は PrimerExplorerV 3（栄研化学）を用いて設計した。各プライマー配列は以下の通り。E 蛋白領域（1237 塩基－1464 塩基）は TBEV-E-1-F3：GCACAGTGTGCAAGAGAGA、TBEV-E-1-B3：AGGACGCTGTTTTTCTTCCA、TBEV-E-1-FIP：CACAAGACGCCTTGACACAGGTGTGATCGAGGCTGGGGTAA、TBEV-E-1-BIP：CAGGACACGTGTATGACGCCAGACGTAATCCCCCGTATGC、TBEV-E-1-LF：CAATGCTGCCTTTTCCAAATAATCC、TBEV-E-1-LB：TTGTGTACACAGTTAAAGTAGAGCC、NS1 蛋白領域（3318 塩基－3515 塩基）は TBEV-NS1-F3：ACCATAAATGCCGACTGTGA、TBEV-NS1-B3：TGCCACCACCATTGAGC、TBEV-NS1-FIP：CGGCAGCACCACTCTGGAATTCGGGGGCTTCTGTGAGGA、TBEV-NS1-BIP：TGCACACTACCTCCAGTGACGTGAATTCATGAACAGGACGTATTT CC、TBEV-NS1-LF：ACCTTGCCACTCTCTGTGG、TBEV-NS1-LB：ACGGGGACAGACTGTTGGTATGC。TBEV Oshima 株全長 cDNA を組み込んだプラスミドをテンプレートとし、反応液 25ul 中に cDNA が 10^{-1}-10^{-5} コピー数含まれるように希釈し、Loopamp® DNA 増幅試薬キット（栄研化学株式会社）を用いて 62.5℃、1 時間の反応を行った。反応の確認はリアルタイム濁度測定装置 LA320C（栄研化学株式会社）を用いて行い、最終反応後にアガロースゲル電気泳動にてラダーの確認および Loopamp®蛍光・目視検出試薬（栄研化学株式会社）の添加により目視で確認した。

ウイルス感染実験は BSL3 実験室で行い、動物実験は長崎大学における動物実験指針に沿って行った。

C. 研究結果

1）Oshima 株感染後の致死率は B6 マウスで 38.1% (n=21) に対して IL-10 KO B6 マウスでは 63.6% (n=22) となった (P=0.0169)。また、致死個体の生存日数は B6 マウスで 14.1±2.3 日に対して IL-10 KO B6 マウスでは 11.5±1.2 日と 3 日程度短くなった（図 1)。

図 1. Oshima 株感染後の致死率

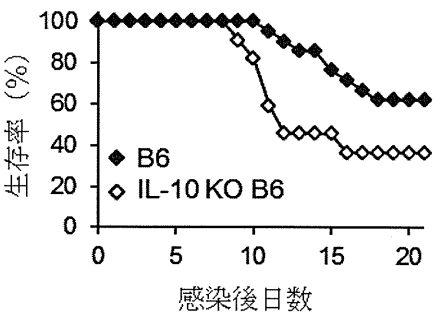

B6 マウス、IL-10 KO B6 マウスともに中枢神経組織内において 5 日目からウイルスが検出されたが、両マウスともにウイルス量に個体間のばらつきがみられた（図 2)。

図 2. Oshima 株感染後のウイルス量

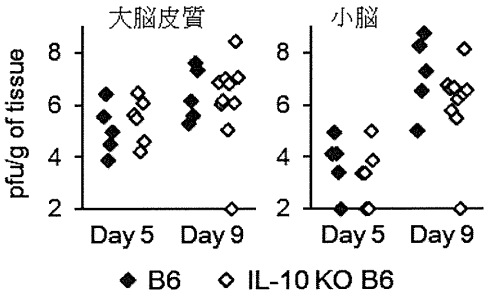

9 日目の中枢神経組織内においても両マウスともにウイルス量に個体間のばらつきがみられたが、B6 マウスと IL-10 KO マウスのあいだにはウイルス量に有意差はみられなかった（大脳皮質 P= 0.8591、小脳 P= 0.5622)（図 2)。

また、IgM と IgG 抗体価は感染 5 日目、9 日目ともに B6 マウスと IL-10 KO マウスのあいだに有意な差は認められなかった。

一方、Sofjin 株感染では B6 マウス、IL-10 KO マウスともに致死率は 100%、致死個体の生存日数は B6 マウスで 9.0±0.3 日、IL-10 KO マウスで 9.4±0.4 日となり両マウス間で差が見られなかった（図 3)。

図 3. Sofjin 株感染後の致死率

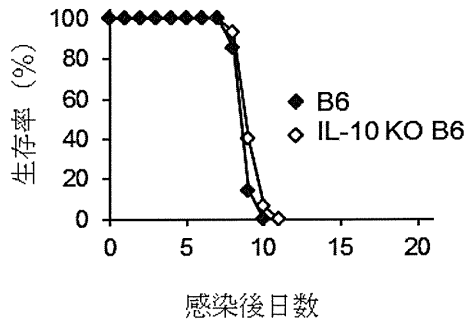

中枢神経組織内のウイルス量は 9 日目において B6 マウス、IL-10 KO マウスともに Oshima 株感染よりも高い値を示したが、B6 マウスと IL-10 KO マウスのあいだに有意な差は認められなかった（大脳皮質 P= 0.4286、小脳 P= 0.6623）（図 4)。

図 4. Sofjin 株感染後のウイルス量

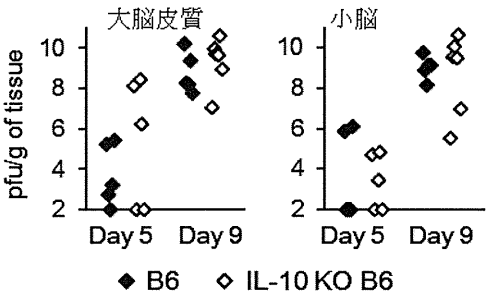

2) LAMP 法により TBEV 遺伝子 cDNA の検出を行った結果、62.5℃、1 時間の反応後に E 蛋白領域、NS1 蛋白領域ともに 10^1 コピー数以上の TBEV 遺伝子の検出が確認された（図 5）。

図 5. 蛍光目視検出試薬による確認

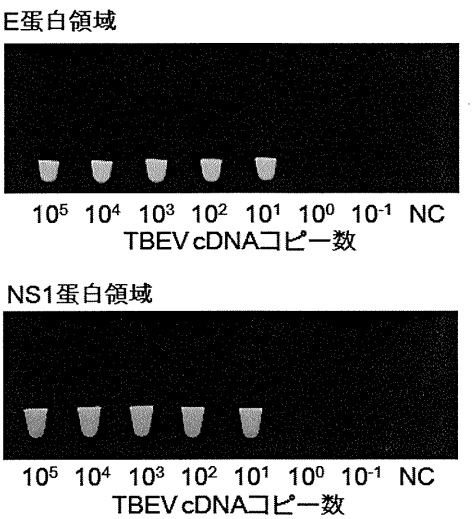

D. 考察

1）TBEV Oshima 株は IL-10 KO マウスへの感染で重症化の亢進がみられたことから、IL-10 応答は重症化を抑える働きがあること

が示唆された。しかしながら、B6 マウスと IL-10 KO マウスにおいて中枢神経組織におけるウイルス量には有意な増加が認められなかったことから、IL-10 KO マウスにおける重症化亢進はウイルスの神経感染の程度のみが要因ではないことが考えられた。IL-10 は免疫応答を抑制するサイトカインであることから、免疫応答すなわち免疫病原性が重症化に関与していることが示唆された。一方、Sofjin 株感染では IL-10 KO でも致死性に違いがみられなかったことから、Sofjin 株感染の場合は IL-10 応答の重症化への関与は小さいものと考えられた。

2）本研究で試みた LAMP 法では 10^1 コピー数までの TBEV 遺伝子を検出できることが確認された。今後、人血清中の TBEV 遺伝子 RNA の検出を試み LAMP 法による迅速簡便診断法の確立を目指す。さらに、マダニ乳剤中に含まれる TBEV 遺伝子 RNA の検出を確認し、TBEV 陽性マダニの迅速簡便検出法を確立することにより、野外採集したマダニの TBEV 保有状況を調査するうえでの有効なアプローチへの応用を目指す。また、今回用いた E 蛋白領域の LAMP プライマーは極東型 TBEV に特異的に、NS1 蛋白領域プライマーは極東型、シベリア型およびヨーロッパ型 TBEV に共通に反応が予想される領域で作製したため、本研究で確立した LAMP 法は TBEV の型分類への応用も期待される。

E. 結論

本研究成果により TBE の重症化には感染個体の免疫応答が関わっていること、IL-10 応答は重症化を抑えていることが示唆された。今後、さらに重症化に関わる免疫応答を詳細に解析し、TBE 重症化を抑える機序を明らかにすることで、TBE 患者に対する特異的かつ有効な治療薬の開発に結びつくことが期待される。

また、今回確立した LAMP 法による TBEV 遺伝子検出系は、TBE 患者の迅速簡便診断法の確立、さらに TBEV 陽性地区特定の有効な検出法の確立へと応用が期待される。

F. 健康危険情報

特になし

G. 研究発表

1. 論文発表

1) Hayasaka D. The Development of encephalitis following Tick-borne encephalitis virus infection in a mouse model. Flavivirus Encephalitis. 2011, Chapter 8, 157-166.

2) Kitaura K, Fujii Y, Hayasaka D, Matsutani T, Shirai K, Nagata N, Lim CK, Suzuki S, Takasaki T, Suzuki R, Kurane I. High Clonality of Virus-Specific T Lymphocytes Defined by TCR Usage in the Brains of mice infected with west nile virus. J Immunol. 2011, 187, 3919-3930.

3) Fujii Y, Hayasaka D, Kitaura K, Takasaki T, Suzuki R, Kurane I. T-cell clones expressing different T-cell receptors accumulate in the brains of dying and surviving mice after peripheral infection with far eastern strain of

tick-borne encephalitis virus. Viral Immunol. 2011, 24, 291-302.

2.学会発表

1) 早坂大輔、藤井克樹、永田典代、堀朋子)、辻百衣璃、北浦一孝、田中香苗、佐多徹太郎、鈴木隆二、森田公一：日本脳炎ウイルス感染後の重症化に関わる IL-10 応答、第46回日本脳炎ウイルス生態学研究会、金沢 (2011, 5)

2) 早坂大輔、藤井克樹、永田典、青木康太郎、堀朋子、辻百衣璃、北浦一孝、田中香苗、佐多徹太郎、鈴木隆二、森田公一：日本脳炎ウイルス感染後の immunopathogenesis (免疫病原性)による重症化：第48回ウイルス学会九州支部総会、門司 (2011, 8)

3) 日本脳炎ウイルス感染性 cDNA クローンの作製および性状解析：高松 由基、ディンティアン デュク、早坂 大輔、森田公一：第48回ウイルス学会九州支部総会、門司 (2011, 8)

4) Daisuke Hayasaka, Yoshiki Fujii, Noriyo Nagata, Kazuki Kitaura, Kanae Tanaka, Tetsutaro Sata, Ryuji Suzuki, Kouichi Morita : Multiple mechanisms for severe form following Japanese encephalitis virus infection : International Union of Microbiological Societies 2011 Congress, Sapporo (2011, 9)

5) 日本脳炎ウイルス感染後の重症化に関わる IL-10 応答：早坂大輔、藤井克樹、永田典代、堀朋子、辻百衣璃、北浦一孝、田中香苗、佐多徹太郎、鈴木隆二、森田公一：第152回日本獣医学会学術集会、堺 (2011,9)

6) 日本脳炎ウイルス感染後の免疫病原性による重症化：早坂大輔、北浦一孝、永田典代、青木康太郎、藤井克樹、鈴木隆二、森田公一：第52回日本熱帯医学会大会、東京 (2011, 11)

7) The Pathogenic mechanisms of Tick-Borne Encephalitis Virus by using IL-10 knock-out mice : Mya Myat Ngwe Tun, Daisuke Hayasaka, Kouichi Morita : 第52回日本熱帯医学会大会、東京 (2011, 11)

8) 日本脳炎ウイルス感染でのTNFα応答の役割：早坂大輔、青木康太郎、Dash Sima Simanti, 田中香苗、森田公一：第17回トガ・フラビ・ペスチウイルス研究会、東京 (2011, 11)

H. 知的財産権の出願・登録状況

なし

1. 特許取得

なし

2. 実用新案登録

なし

3. その他

なし

III. 研究成果の刊行に関する一覧表

発表者氏名	論文タイトル名	発表誌名	巻　号	ページ	出版年
Yoshii, K., Mottate, K., Omori-Urabe, Y., Chiba, Y., Seto, T., Sanada, T., Maeda, J., Obara, M., Ando, S., Ito, N., Sugiyama, M., Sato, H., Fukushima, H., Kariwa, H., Takashima, I.	Epizootiological Study of Tick-Borne Encephalitis Virus Infection in Japan.	J. Vet. Med. Sci.	73 (3)	409-412	2011
Yoshii, K., Igarashi, M., Ito, K., Kariwa, H., Holbrook, M.R., Takashima, I.	Construction of an infectious cDNA clone for Omsk hemorrhagic fever virus, and characterization of mutations in NS2A and NS5.	Virus Res.	155 (1)	61-68	2011
Seto, T., Tkachenko, E.A., Morozov, V.G., Tanikawa, Y., Kolominov, S.I., Belov, S.N., Nakamura, I., Hashimoto, N., Kon, Y., Balakiev, A.E., Dzagurnova, T.K., Medvedkina, O.A., Nakauchi, M., Ishizuka, M., Yoshii, K., Yoshimatsu, K., Ivanov, L.V., Arikawa, J., Takashima, I., Kariwa, H.	An Efficient in vivo Method for the Isolation of Puumala Virus in Syrian Hamsters and the Characterization of the isolates from russia.	J. Virol. Methods.	173 (1)	17-23	2011
Ikawa-Yoshida, A., Yoshii, K., Kuwahara, K., Obara, M., Kariwa, H., Takashima, I.	Development of ELISA system for tick-borne encephalitis virus infection in rodents.	Microbiol. Immunol.	55 (2)	100-107	2011
Murata, R., Hashiguchi, K., Yoshii, K., Kariwa, H., Nakajima, K., Ivanov, L.I., Leonova, G.N., Takashima, I.	Seroprevalence of West Nile Virus in Wild Birds in Far Eastern Russia Using a Focus Reduction Neutralization Test.	Am. J. Trop. Med. Hyg.	84 (3)	461-465	2011
Sanada, T., Kariwa, H., Nagata, N., Tanikawa, Y., Seto, T., Yoshimatsu, K., Arikawa, J., Yoshii, K., Takashima, I.	Puumala virus infection in Syrian hamsters (Mesocricetus auratus) resembling hantavirus infection in natural rodent hosts.	Virus Res.	160 (1-2)	108-119	2011
Totani, M.., Yoshii, K., Kariwa, H., Takashima, I.	Glycosylation of the Envelope Protein of West Nile Virus Affects Its Replication in Chicks.	Avian Diseases	55 (4)	561-568	2011
Takano, A.., Yoshii, K., Omori-Urabe, Y., Yokozawa, K., Kariwa, H., Takashima, I.	Construction of a replicon and an infectious cDNA clone of the Sofjin strain of the Far-Eastern subtype of tick-borne encephalitis virus.	Arch. Virol.	156 (11)	1931-1941	2011
Obara, M., Yamauchi, T., Watanabe, M., Hasegawa, S., Ueda, Y., Matsuno, K., Iwai, M., Horimoto, E., Kurata, T., Takizawa, T., Kariwa, H., Takashima, I.	Continuity and change of Japanese encephalitis virus in Toyama Prefecture, Japan.	Am. J. Trop. Med. Hyg..	84 (5)	695-708	2011
Gamage, C.D., Yasuda, S.P., Nishio, S., Kularatne, S.A., Weerakoon, K., Rajapakse, J., Nwafor-Okoli, C., Lee, R.B., Obayashi, Y., Yoshimatsu, K., Arikawa, J., Tamashiro, H.	Serological evidence of Thailand virus-related hantavirus infection among suspected leptospirosis patients in Kandy, Sri Lanka.	Jpn. J. Infect. Dis.	64 (1)	72-75.	2011
Yasuda, S.P., Yoshimatsu, K., Koma, T., Shimizu, K., Endo, R., Isozumi, R., Arikawa, J.	Application of truncated nucleocapsid protein (N) for serotyping ELISA of Murinae-associated hantavirus infection in rats.	J. Vet. Med. Sci.	74	215-19	2012
Taniguchi S, Watanabe S, Masangkay JS, Omatsu T, Ikegami T, Alviola P, Ueda N, Iha K, Fujii H, Ishii Y, Mizutani T, Fukushi S, Saijo M, Kurane I, Kyuwa S, Akashi H, Yoshikawa Y, Morikawa S.	Reston Ebolavirus antibodies in bats, the Philippines.	Emerg. Infect. Dis.	17 (8)	1559-1560	2011
Ito, N., Mita, T., Shimizu, K., Ito, Y., Masatani, T., Nakagawa, K., Yamaoka, S., Abe, M., Okadera, K.,	Amino Acid substitution at position 95 in rabies virus matrix protein affects viral pathogenicity.	J. Vet. Med. Sci.	73(10)	1363-1366	2011

Kaku Y, Noguchi A, Hotta K, Yamada A, Inoue S.	Inhibition of rabies virus propagation in mouse neuroblastoma cells by an intrabody against the viral phosphoprotein.	Antiviral Res.	91(1)	64-71	2011
Nguyen, A.K., Nguyen, D.V., Ngo, G.C., Nguyen, T.T., Inoue, S., Yamada, A., Dinh, X.K., Nguyen, DV, Phan, T.X., Pham, B.Q., Nguyen, H.T., Nguyen, H.T.	Molecular epidemiology of rabies virus in Vietnam (2006-2009).	Jpn. J. Infect. Dis.	64(5)	391-396	2011
Sugiura, N., Uda, A., Inoue, S., Kojima, D., Hamamoto, N., Kaku, Y., Okutani, A., Noguchi, A., Park, C.H., Yamada, A.	Gene expression analysis of host innate immune responses in the central nervous system following lethal CVS-11 infection in mice.	Jpn. J. Infect. Dis.	64(6)	463-72.	2011
Kitaura, K., Fujii, Y., Hayasaka, D., Matsutani, T., Shirai, K., Nagata, N., Lim, C.K., Suzuki, S., Takasaki, T., Suzuki, R., Kurane, I.	High Clonality of Virus-Specific T Lymphocytes Defined by TCR Usage in the Brains of mice infected with west nile virus.	J. Immunol.	187 (8)	3919-3930	2011
Fujii, Y., Hayasaka, D., Kitaura, K., Takasaki, T., Suzuki, R., Kurane, I.	T-cell clones expressing different T-cell receptors accumulate in the brains of dying and surviving mice after peripheral infection with far eastern strain of tick-borne encephalitis virus	Viral Immunol.	24 (4)	291-302	2011
Kabeya, H., Inoue, K., Izumi, Y., Morita, T., Imai, S., Maruyama, S.	Bartonella species in wild rodents and the infested fleas in Japan.	J. Vet. Med. Sci.	73 (2)	1561-1567	2011
Lee, K., Iwata, T., Nakadai, A., Kato, T., Hayama, S., Taniguchi, T., Hayashidani, H.	Prevalence of Salmonella, Yersinia and Campylobacter spp. in feral raccoons (Procyon lotor) and masked palm civets (Paguma larvata) in Japan.	Zoonoses Public Health	58 (6)	424-31	2011

IV. 研究成果の刊行物・印刷

Virus Research 155 (2011) 61–68

Contents lists available at ScienceDirect

Virus Research

journal homepage: www.elsevier.com/locate/virusres

Construction of an infectious cDNA clone for Omsk hemorrhagic fever virus, and characterization of mutations in NS2A and NS5

Kentaro Yoshii[a,b,*], Manabu Igarashi[c], Kimihito Ito[c], Hiroaki Kariwa[a], Michael R. Holbrook[b,d], Ikuo Takashima[a]

[a] Laboratory of Public Health, Graduate School of Veterinary Medicine, Hokkaido University, Sapporo, Hokkaido 060-0818, Japan
[b] Department of Pathology, Institute for Human Infections and Immunity, University of Texas Medical Branch, Galveston, TX 77555, USA
[c] Department of Global Epidemiology, Hokkaido University Research Center for Zoonosis Control, Sapporo 001-0020, Japan
[d] NIAID Integrated Research Facility, Frederick, MD 21702, USA

ARTICLE INFO

Article history:
Received 29 June 2010
Received in revised form 26 August 2010
Accepted 26 August 2010
Available online 15 September 2010

Keywords:
Omsk hemorrhagic fever
Flavivirus
Infectious cDNA
Viral replication

ABSTRACT

Omsk hemorrhagic fever virus (OHFV) is a member of the tick-borne encephalitis serocomplex of flaviviruses, and causes hemorrhagic disease in humans. In this study, an infectious cDNA of OHFV was constructed to investigate the molecular mechanisms involved in OHFV pathogenesis for the first time. Our cDNA clone was capable of producing infectious virus which is genetically identical to the parental Guriev strain, and the recombinant virus showed similar biological properties to the parental virus including growth kinetics and virulence characteristics. While characterizing the cDNAs, fortuitous mutations at NS2A position 46 and NS5 position 836 were found to affect viral production. By using a viral replicon expressing luciferase, it was shown that both of the mutations produced a defect in RNA replication and that the NS5 mutation induced a temperature-sensitive phenotype, indicating the importance of these residues in RNA replication. This infectious cDNA will be a useful tool to study the replication and pathogenesis of OHFV.

1. Introduction

Omsk hemorrhagic fever (OHF) is a disease caused by Omsk hemorrhagic fever virus (OHFV), which belongs to the tick-borne encephalitis (TBE) serocomplex, genus *Flavivirus*, family *Flaviviridae*. OHFV was first isolated in 1947 from a human presenting with hemorrhagic fever. OHFV is endemic to a fairly localized region of Siberia within the Omsk and Novosibirsk Oblasts in Russia (Burke and Monath, 2001). OHFV is transmitted via the bite of its primary tick vector, *Dermacentor reticulates*. The transmission cycle of OHFV involves water voles (*Arvicola terrestris*) and muskrats (*Ondata zibethica*), and many other animals within endemic area can be infected with OHFV (Busygin, 2000; Kharitonova and Leonov, 1985).

The TBE complex includes tick-borne encephalitis virus (TBEV), Powassan virus, Langat virus (LGTV), Louping ill virus, OHFV, Alkhurma virus (ALKV), and Kyasanur Forest disease virus (KFDV) (Buchen-Osmond, 2003). Although the TBE complex is largely represented by viruses causing encephalitis, OHFV, ALKV and KFDV are known to cause hemorrhagic disease. Unlike ALKV and KFDV, OHFV causes a hemorrhagic disease in humans with few neurological effects (Burke and Monath, 2001). Human OHFV infection results in fever, headache, myalgia, dehydration, and hemorrhage. The mortality rate for OHF is estimated to be 0.4–2.5% (Kharitonova and Leonov, 1985). In the mouse model, OHFV causes disease with few neurological signs compared to neurotropic tick-borne flaviviruses and has also demonstrated significantly different tissue localization indicating potential differences in host cell interactions (Holbrook et al., 2005). However, the specific viral and host response mechanisms involved in OHFV pathogenesis are not well understood.

The flavivirus genome consists of a positive-polarity, single-stranded RNA of approximately 11 kb, which encodes three structural proteins, i.e., the core (C), premembrane (prM), and envelope (E) proteins, and seven non-structural (NS) proteins (NS1, NS2A, NS2B, NS3, NS4A, NS4B, and NS5), within a single long open reading frame (Chambers et al., 1990). The 5′- and 3′-UTRs have predicted secondary structures that are implicated in viral replication, translation, and packaging of the genomes (Gritsun et al., 1997; Proutski et al., 1997; Rauscher et al., 1997).

Abbreviations: OHF, Omsk hemorrhagic fever; OHFV, Omsk hemorrhagic fever virus; TBE, tick-borne encephalitis; LGTV, Langat virus; ALKV, Alkhurma virus; KFDV, Kyasanur Forest disease virus; C, core; prM, premembrane; E, envelope; NS, non-structural; HDV-RZ, hepatitis delta virus ribozyme; MOI, multiplicity of infection; RdRp, RNA-dependent RNA polymerase; EM, energy minimization; rms, root mean square; ts, temperature-sensitive; NLS, nuclear localization sequence.

* Corresponding author at: Laboratory of Public Health, Graduate School of Veterinary Medicine, Hokkaido University, kita-18 nishi-9, kita-ku, Sapporo, Hokkaido 060-0818, Japan. Tel.: +81 11 706 5213; fax: +81 11 706 5213.
E-mail address: kyoshii@vetmed.hokudai.ac.jp (K. Yoshii).

0168-1702/$ – see front matter © 2010 Elsevier B.V. All rights reserved.
doi:10.1016/j.virusres.2010.08.023

Infectious cDNA clones have been generated for multiple flaviviruses, and they provide a useful platform on which to investigate the genetic determinants of flavivirus virulence. There are several reports of infectious cDNA clones for TBE serocomplex, TBEV and LGTV (Campbell and Pletnev, 2000; Gritsun and Gould, 1998; Hayasaka et al., 2004; Mandl et al., 1997; Pletnev, 2001). However, an infectious clone has not been developed for OHFV. In this study, we report the construction and characterization of an infectious cDNA clone of OHFV. Furthermore, while characterizing this cDNA, several fortuitous mutations in NS proteins were shown to attenuate viral replication and reduce virulence in mice.

2. Materials and methods

2.1. Cell and virus

BHK cells were grown in MEM supplemented with 8% FBS. OHFV strain Guriev was obtained from the World Reference Collection for Emerging Viruses and Arboviruses (WRCEVA) and used for construction of the infectious cDNA clone.

2.2. Plasmid constructions

Total cellular RNA was extracted from OHFV (strain Guriev)-infected BHK cells using Trizol (Invitrogen). OHFV RNA was reverse-transcribed with specific oligonucleotide primers using Superscript II reverse transcriptase (Invitrogen). The fragments of OHFV cDNA were amplified by *Platinum Taq* polymerase (Invitrogen) using specific oligonucleotide primers (see Fig. 1), resolved by gel electrophoresis and purified using the Qiaquick gel extraction kit (Qiagen).

The resulting fragments were digested with restriction endonucleases and cloned into the low copy plasmid pACNR provided by Dr. Peter Mason (Ruggli et al., 1996) as depicted in Fig. 1. The oligonucleotide used to amplify the 5′UTR included a T7 promoter recognition site and an additional G preceding the first base of the viral genome. A synthetic oligonucleotide was used to add Cla I site at nucleotides 2436–2441. This silent mutation was engineered to permit the ligation of the fragment containing the structural protein gene. A hepatitis delta virus ribozyme (HDV-RZ)/bacteriophage T7 terminator fragment (Mason et al., 2002) was fused to the 3′ end of the viral genome to create synthetic run-off transcripts that contained a 3′ terminus identical to the viral RNA. The resulting cloned plasmids (designated as OHF-IC) were isolated by standard techniques and sequences were checked at the University of Texas Medical Branch (UTMB) Protein Chemistry Laboratory and compared to the sequence of the original OHFV Guriev sequence (accession No. AB507800). Sequencing identified three mutations encoding amino acid changes at NS2A-46, NS5-65 and NS5-836.

To repair the mutations found in the OHF-IC plasmids, the fragments between nucleotide 3612–3685 (Hpa I–Sph I site), 7094–8778 (Bam HI–Kpn I site), 9488–10295 (Nde I–Apa I site) were amplified by RT-PCR and subsequently cloned into pCR2.1 plasmid (TA cloning kit; Invitrogen). The virus-specific sequence of each intermediate cloning product was checked by sequence analysis. These intermediate plasmids containing the correct sequence were cut by restriction enzymes described above and used to substitute the regions containing the mutations.

Subgenomic OHFV replicons expressing luciferase gene (OHF-REP-luc (Yoshii and Holbrook, 2009)) were used to analyze the effect of the mutations on viral genome replication. Fragments from the mutated OHF-IC plasmids were amplified using the same primers sets described above. The PCR product from the fragments containing mutations was cloned into the replicon plasmid to generate replicons containing the specific mutations found in OHF-IC.

2.3. RNA synthesis-transfection

The RNAs were synthesized as described previously (Yoshii et al., 2005). Briefly, the plasmids were prepared for run-off transcription by digestion with XbaI restriction endonuclease, and the resulting template DNAs were in vitro transcribed using the mMESSAGE mMACHINE T7 Kit (Ambion) in a 20-μl reaction mixture that contained an additional 1 μl of 20 mM GTP solution. After transcription at 37 °C for 2 h, the template DNAs were removed by DNase I digestion at 37 °C for 15 min. The RNA was precipitated using lithium chloride, washed with 70% ethanol, resuspended in RNase-free water, quantitated by spectrophotometer, and stored at −80 °C in aliquots. The synthesized RNA was transfected into BHK cells using TransIT-mRNA (Mirus Bio) by a slight modification of the manufacturer's protocol.

2.4. Detection of OHFV-antigen (IFA)

Cells were fixed with 3% paraformaldehyde, and permeabilized with 0.2% Triton X-100. After blocking with 2% BSA, the cells were incubated with Rabbit polyclonal antibodies against TBEV E proteins which is cross-reactive to OHFV E proteins (Yoshii et al., 2004), and then treated with Alexa 555-conjugated anti-rabbit IgG antibodies (Invitrogen). The images were viewed and recorded using fluorescence microscopy.

2.5. Viral titration and growth curves

Stock preparations of recombinant OHFV from OHF-IC were produced by passaging the virus harvested from the supernatant of RNA-transfected cells once in BHK cells. The sequence of the RNA of the recovered stock virus was confirmed to be identical to that of the each OHF-IC plasmid by sequence analysis after RT-PCR. For titrations, cell monolayers prepared in multi-well plates were incubated with serial dilutions of virus for 1 h, and then overlaid with MEM containing 2% FBS and 1.5% carboxymethyl cellulose (CMC; Sigma) and incubated for 5 days. After incubation, the cells were fixed and stained with 0.25% crystal violet in 10% buffered formalin. Plaques were counted and expressed as p.f.u./ml. For growth curves, BHK cells were infected at a multiplicity of infection (MOI) of 0.01. After virus adsorption for 1 h, the inocula were removed, and the cells were washed with PBS and incubated in MEM containing 2% FBS. The media was harvested at 24, 48, 72, 96 h post-infection and stored at −80 °C.

2.6. Luciferase assay

For preparation of cell extracts for luciferase assays, BHK cells were washed with PBS and lysed by the addition of cell culture Reporter lysis buffer (Promega), followed by the incubation of cells at room temperature for 10 min. The cell extracts were then harvested and stored at −80 °C. Luciferase assays were carried out using Luciferase Assay System (Promega) according to manufacturer instructions, and luminescence was determined using a Microplate Luminometer.

2.7. Virulence in mice

Eight-week-old female C57BL/6J mice (Charles River Japan, Inc.) were challenged with 1000 p.f.u. of each virus subcutaneously in the dorsal region. The physical conditions of the mice were observed and the body weight was measured daily. All procedures were according to the guidelines of the Animal Care and Use Committee of the Hokkaido University.

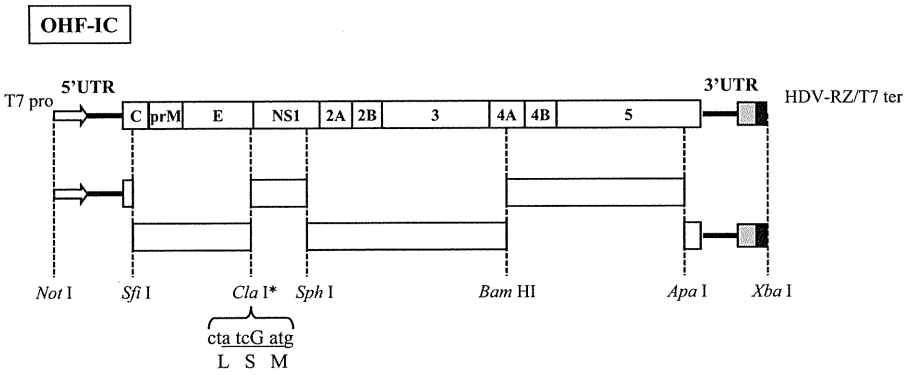

Fig. 1. Construction of the full-length infectious clone of OHFV. Six cDNA fragments synthesized by RT-PCR were assembled to form the full-length cDNA clone of OHFV (OHF-IC). Restriction sites used to construct OHF-IC are shown at the bottom. A silent mutation (shown in uppercase) was engineered to create a Cla I site (*). The complete OHFV cDNA is positioned under the control of the T7 promoter. A hepatitis delta virus ribozyme (HDV-RZ)/bacteriophage T7 terminator fragment was fused to the 3′ end of the viral genome (see Section 2).

2.8. Molecular modeling

A homology model of OHFV RNA-dependent RNA polymerase (RdRp) domain was constructed based on the crystal structure of the dengue virus RdRp domain (PDB code, 2J7W, sequence identity: ca 61%). MODELLER 9v6 (Eswar et al., 2003) was used for homology modeling of OHFV RdRp domains. After 100 models of the RdRp domain were generated, a model was chosen by the MODELLER objective function value. After addition of hydrogen atoms, the model was refined by energy minimization (EM) using CHARMm force field with the Discovery Studio 2.1 software package (Accelrys, San Diego, CA). Steepest descent followed by conjugate gradient minimizations was carried out until the root mean square (rms) gradient was less than or equal to 0.05 kcal/mol/A. The generalized Born implicit solvent model (Still et al., 1990; Tsui and Case, 2000) was used to model the effects of solvation. The molecular model was finally evaluated by using PROCHECK (Laskowski et al., 1993) and VERIFY-3D (Eisenberg et al., 1997). The model structure was displayed by PyMOL (DeLano Scientific LLC) (DeLano, 2002).

3. Results

3.1. The construction of the full-length infectious clone of OHFV

The overall strategy to construct the full-length infectious clone of OHFV strain Guriev is outlined in Fig. 1. The viral RNA was extracted from infected BHK cells, and individual dsDNA fragments were amplified by RT-PCR, as shown Fig. 1. The six individual fragments were readily assembled into the low-copy plasmid pACNR, which has been used successfully to construct stable infectious clones in several flaviviruses (Bredenbeek et al., 2003; McElroy et al., 2005; Rossi et al., 2005). The complete genome sequence of this plasmid (designated OHF-IC-ori) was determined and compared with the parent virus. There were 10 nucleotide differences with three resulting in amino acid changes, one in NS2A and two in NS5 (Table 1). An additional nucleotide change was intentionally designed to create a ClaI site (C to G at nt 2439). This restriction site was used for the cloning of the DNA fragment between nt 135 and 2441. The other mutations were caused by PCR steps during the amplification of each fragment. These mutations were repaired by substitution as described in Section 2, and the infectious clone of OHFV, which is genetically identical to the parent virus Guriev, was obtained and designated as OHF-IC-pt. These OHF-IC plasmids were found to be stable during transformations into *E. coli* and large-scale plasmid production. After several bacterial passages, the sequence of the plasmid was identical.

Table 1
Summary of sequence difference between the infectious cDNA OHF-IC-ori and parental OHFV strain Guriev.

Base position[a]	Strain Guriev	OHF-IC-ori	Amino acid change	Location
297	A	G	–	
2367	G	A	–	
2439	C	G[b]	–	
3653	T	A	L→H	$NS2A_{46}$[c]
6231	C	T	–	
6591	A	T	–	
6678	T	C	–	
7859	T	C	L→P	$NS5_{65}$
7983	A	G	–	
10172	A	G	D→G	$NS5_{836}$

[a] Nucleotide position and sequence are based on OHFV strain Guriev (Accession no. AB507800).
[b] This silent mutation (shown in uppercase) was engineered to create a Cla I site (*).
[c] The numbers indicate the amino acid position in each protein.

3.2. Generation of OHFV from infectious clone

XbaI-linearized OHF-IC template was used for *in vitro* RNA transcription using T7 RNA polymerase and the resulting full-length OHFV transcripts were transfected into BHK cells. At 5 days post-transfection, the transfected cells were fixed and the expression of virus proteins was analyzed by immunofluorescence assay. Most of the cells transfected with the transcripts from OHF-IC-pt showed a perinuclear signal when stained with an E-specific antibody (Fig. 3A). Infectious virus could be harvested from the supernatants

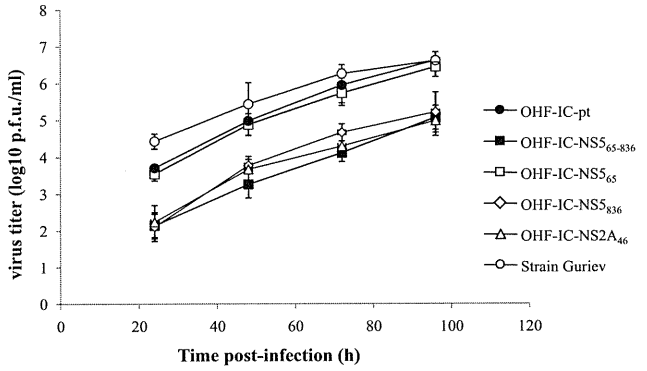

Fig. 2. Immunofluorescence staining of BHK cells transfected with the *in vitro* transcript of OHF-IC-pt (A) and OHF-IC-ori (B). Cells were fixed at 5 days post-transfection and stained with MAb 1H4.

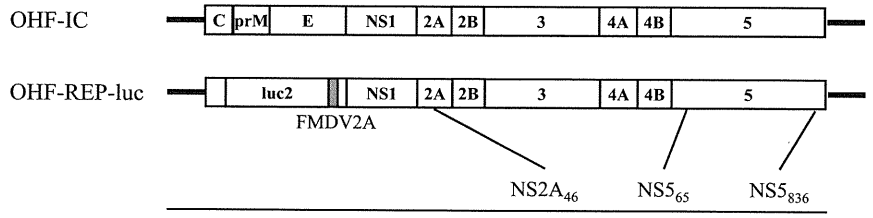

	$NS2A_{46}$	$NS5_{65}$	$NS5_{836}$
Parental virus (strain Guriev)	**L**	**L**	**D**
OHF-IC-ori	H	P	G
OHF-IC-$NS5_{65-836}$ OHF-REP-luc-$NS5_{65-836}$	**L**	P	G
OHF-IC-$NS5_{65}$ OHF-REP-luc-$NS5_{65}$	**L**	P	**D**
OHF-IC-$NS5_{836}$ OHF-REP-luc-$NS5_{836}$	**L**	**L**	G
OHF-IC-$NS2A_{46}$ OHF-REP-luc-$NS2A_{46}$	H	**L**	**D**
OHF-IC-pt OHF-REP-luc	**L**	**L**	**D**

Fig. 3. Growth curves of parental Guriev, OHF-IC-pt, OHF-IC-$NS5_{65}$, OHF-IC-$NS5_{836}$, OHF-IC-$NS5_{65-836}$, and OHF-IC-$NS2A_{46}$. A Monolayer of BHK cells was infected with the individual viruses at a multiplicity of infection (MOI) of 0.01. At each time point, the media was harvested and virus titers were determined by plaque assay in BHK cells.

of the transfected cells, and a cytopathic effect was observed in these cell cultures. However no infectious virus could be recovered from cells transfected with RNAs from OHF-IC-ori, and no virus antigens were observed in the cells by immunofluorescence assay (Fig. 3B). These data indicated two things: the production of viral proteins in the cells transfected with RNAs from OHF-IC-pt was not merely the result of translation of the input RNA, and the mutations in OHF-IC-ori affected the production of viral proteins and infectious viruses.

The growth properties of OHF-IC-pt derived virus and wild-type OHFV were analyzed by monitoring the release of virus after infection. BHK cells were infected at m.o.i. of 0.01 with OHFV. Virus was harvested at 24 h intervals and the yield was quantified by plaque assay (Fig. 4). There was slight difference in the yields of virus at 24 h post-infection, but the resulting growth curves indicate similar growth properties between the parent virus and recombinant virus from OHF-IC-pt. The slight difference at 24 h post-infection may derive from the quasispecies of the parent virus stock because the virus was not plaque purified.

3.3. Characterization of NS mutant

To determine how the mutations in OHF-IC-ori affected the viral production from the OHFV infectious cDNAs, we prepared several infectious cDNAs that incorporated the mutations identified in OHF-IC-ori (Fig. 2). The OHF-IC-$NS5_{65-836}$, OHF-IC-$NS5_{65}$ and OHF-IC-$NS5_{836}$ plasmids have the NS5 mutations, and OHF-IC-$NS2A_{46}$ has the NS2A mutation. Recombinant viruses were recovered from these infectious cDNAs, and the growth curves were generated as described above.

No significant differences were observed between the growth curves of OHF-IC-pt and OHF-IC-$NS5_{65}$ (Fig. 4), indicating that the amino acid difference at NS5 position 65 (L to P) did not affect virus growth in BHK cells. Meanwhile, the growth of OHF-IC-$NS2A_{46}$, OHF-IC-$NS5_{65-836}$ and OHF-IC-$NS5_{836}$ was restricted relative to OHF-IC-pt and OHF-IC-$NS5_{65}$. These results indicate that the mutations at NS2A position 46 (L to H) and NS5 position 836 (D to G) limited the virus growth in cell culture.

To further investigate the effect of the NS2A and NS5 mutations on virus production, we prepared a replicon of OHFV containing the luciferase reporter gene with or without the NS mutations (see Section 2 and Fig. 2). These replicon RNAs were transfected into BHK cells, and luciferase activities were measured at 6 h and 3 days post-transfection. There was no difference between the luciferase activities of the replicons at 6 h post-transfection (Fig. 5A), indicating that the mutations had no effect on the initial translation of reporter gene from transfected replicon RNA. At 3 days post-transfection, the luciferase activity was lower in the lysate from the replicons with mutations at NS2A position 46 or NS5 position 836 at 37 °C (Fig. 5B). In contrast, there was no decrease in luciferase activities was detected in the lysates from the replicon with and without the mutation at NS5 position 836 at 30 °C. Luciferase activity in cells transfected with the replicon containing the NS2A-46 mutation remained diminished in cells incubated at 30 °C. Similar temperature sensitivity of NS5-836 was observed in the virus production at 30 °C (supplementary Fig. 1). These data indicate that the mutations at NS2A-46 and NS5-836 reduce viral replication by reducing RNA replication and that the NS5-836 mutation produces a temperature-sensitive (ts) defect in RNA replication.

3.4. Pathogenicity of infectious clone-derived viruses in mouse model

In our previous studies, we described that laboratory mice infected with OHFV showed clinical signs and pathology similar to reports of human infection (Holbrook et al., 2005; Tigabu et al., 2009). The pathogenicity of recombinant viruses was examined in the mouse model. Five adult C57BL/6 mice were infected subcutaneously with 1000 p.f.u. of each virus and survival was recorded for 28 days (Fig. 6).

OHF-IC-pt virus which is genetically identical to parental OHFV Guriev strain produced 100% mortality of mice (mean survival

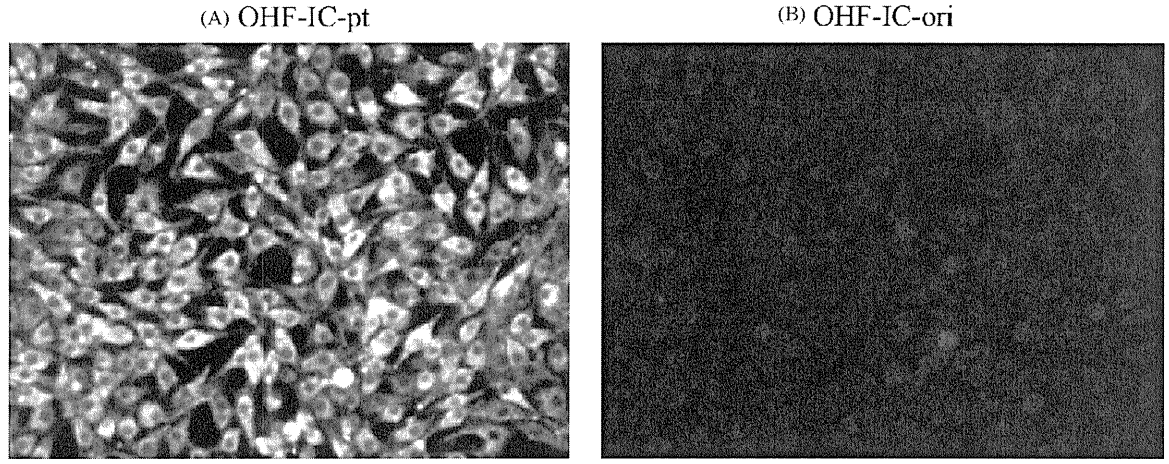

Fig. 4. Schematic representation of the genome of OHFV showing all of the amino acid coding difference between strain Guriev and constructed full-length clones (OHF-IC) and OHFV replicons used to analyze the effect of NS2A and NS5 mutations. Bold type has been used to designate the amino acids of the consensus sequence in Guriev (see text and Table 1).

time 13.8 ± 1.92). All mice showed general signs of illness such as hunched posture, ruffled fur, and general malaise, but did not have significant or consistent indications of neurologic disease. After onset of disease, they showed a sharp decrease in body weight beginning at 9 and 10 dpi. When examined postmortem, all mice had conjunctival suffusion with crusting and some had bowel hemorrhage. These results were consistent with our previous data in which mice infected with parental OHFV Guriev strain had viscerotropic disease with limited signs of neurological disease (100% mortality and mean survival time 12.8 ± 2.49) (Tigabu et al., 2009).

The OHF-IC-NS5$_{65}$ virus had similar virulence to the OHF-IC-pt virus (100% mortality and mean survival time 14.2 ± 1.92) indicating that the amino acid difference at NS5 position 65 did not affect the biological properties of OHFV confirming observations from *in vitro* studies. However, the OHF-IC-NS2A$_{46}$, OHF-IC-NS5$_{65-836}$ and OHF-IC-NS5$_{836}$ virus showed decreased virulence. The OHF-IC-NS5$_{65-836}$ and OHF-IC-NS5$_{836}$ virus killed three mice, but survival time was increased while the OHF-IC-NS2A$_{46}$ virus was completely attenuated. The NS5-836 mutation was retained in the dead mice inoculated with The OHF-IC-NS5$_{65-836}$ and OHF-IC-NS5$_{836}$ virus. All surviving mice inoculated with the OHF-IC-NS2A$_{46}$, OHF-IC-NS5$_{65-836}$ and OHF-IC-NS5$_{836}$ virus showed no signs of illness and no weight loss. These results indicate that the mutations at NS2A position 46 and NS5 position 836 affect OHFV virulence in association with the lower viral replication. All surviving mice inoculated with OHF-IC-NS2A$_{46}$, OHF-IC-NS5$_{65-836}$ and OHF-IC-NS5$_{836}$ had neutralizing antibody against OHFV (≥320 in 50% reduction), indicating that the virus was able to replicate at the initial stage of infection without causing a disease.

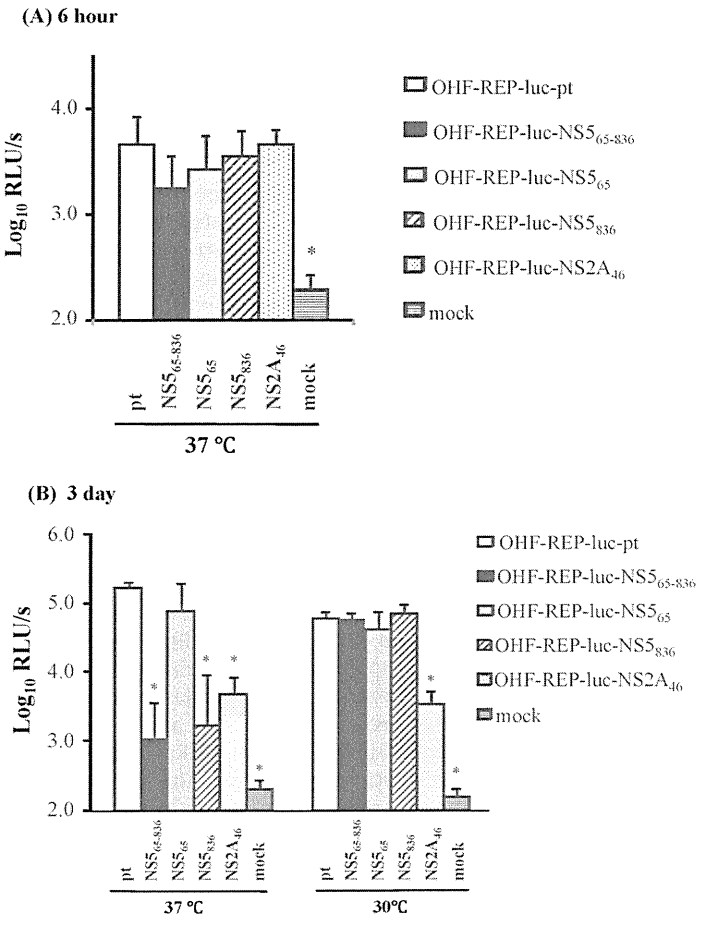

Fig. 5. Effect of NS mutations on OHFV RNA replication. BHK cells were transfected with luciferase-expressing OHFV subgenomic replicon RNAs (OHF-REP-luc) with or without the NS2A or NS5 mutations, and incubated at 37 °C or 30 °C. Luciferase activities were measured at 6 h (A) 72 h (B) post-transfection. Luciferase activities are expressed in Raw Light Units (RLU). Asterisks show the statistically significant difference compared to OHF-REP-luc-pt by Student *T* test ($P < 0.05$).

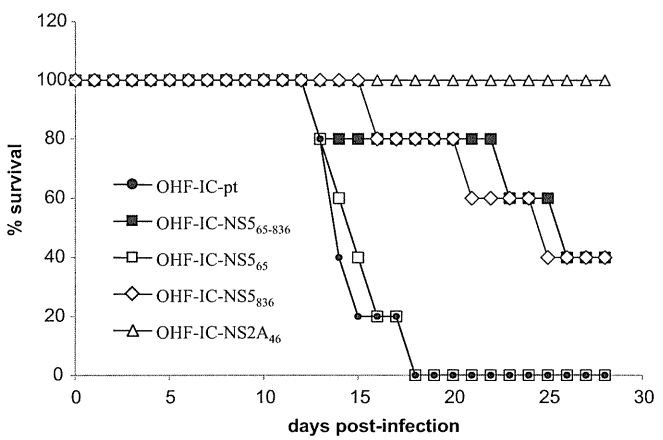

Fig. 6. Survival of mice inoculated with OHF-IC. Mice were inoculated subcutaneously with 1000 p.f.u. of OHF-IC-pt, OHF-IC-NS5$_{65}$, OHF-IC-NS5$_{836}$, OHF-IC-NS5$_{65-836}$, and OHF-IC-NS2A$_{46}$.

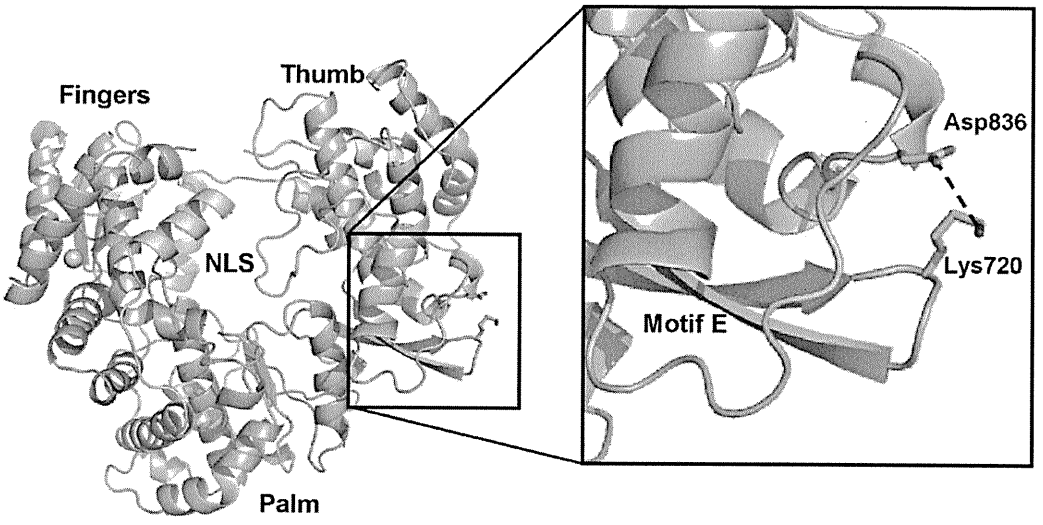

Fig. 7. Location of amino acid substitutions at Asp836 on a homology model of the OHFV RNA-dependent RNA polymerase domain in NS5 based on that of dengue virus (PDB 2J7W). The zoomed region in the right panel shows the proposed interaction of charged side chains between Asp836 and Lys720.

4. Discussion

This is the first report of generation of an infectious clone of OHFV. Infectious clones can be a valuable tool for studying the molecular biology of virus replication, virus structure, virulence determinants, and vaccine development. There is a common difficulty in the construction of full-length clones of flaviviruses, because the plasmids containing a full-length cDNA of these viruses are often unstable during propagation in *E. coli*. Therefore, by using low-copy-number plasmids and specific bacterial hosts, stable full-length infectious clones have been developed for several flaviviruses (Gritsun and Gould, 1998; Hayasaka et al., 2004; Kinney et al., 1997; Mandl et al., 1997; Shi et al., 2002; Yamshchikov et al., 2001; Yun et al., 2003). In this study, the low-copy-number plasmid pACNR was used for the construction of the full-length OHFV cDNA. This vector has been used to construct stable infectious clones of several flaviviruses and pestiviruses (Bredenbeek et al., 2003; McElroy et al., 2005; Mendez et al., 1998; Ruggli et al., 1996). The OHF-IC plasmids were stable during passaging in bacteria, indicating that this infectious clone can be useful for genetic manipulations.

The Guriev strain, which was isolated from human blood, was selected to construct a full-length infectious clone. We previously demonstrated the similarity between human and murine infection with OHFV (Holbrook et al., 2005; Tigabu et al., 2009). The OHFV-infected mice had no indication of neurological problems, and had conjunctival suffusion that has also been reported in human cases. The recombinant virus which is genetically identical to the parental Guriev strain showed similar biological properties to the parental virus, including growth kinetics and virulence characteristics. These results indicate that an efficient reverse genetics system has been established for OHFV.

Our results have identified two amino acid codon substitutions associated with attenuation of the virus production, i.e., Leu46 to His in the NS2A, and Asp836 to Gly in NS5. These substitutions decreased the efficiency of RNA replication, leading to limited virus propagation and decreased virulence in mice.

Flavivirus NS2A is a small, hydrophobic, membrane associated protein involved in RNA replication. It was reported that NS2A binds with high specificity to the 3′ untranslated region (UTR) of viral genomic RNA and to other components of the replication complex (Mackenzie et al., 1998). In addition, NS2A is considered to play roles in modulating the host-antiviral interferon response (Liu et al., 2004, 2006, 2005; Munoz-Jordan et al., 2003) and assembly/secretion processes of virus particles (Kummerer and Rice, 2002; Leung et al., 2008; Liu et al., 2003). Although the exact membrane topology of NS2A is yet to be determined, NS2A of OHFV has been predicted to span the membrane of the endoplasmic reticulum five times by several transmembrane domain prediction programs (TMHMM (Krogh et al., 2001), and TMpred (Hofmann and Stoffel, 1993)). The Leu46 residue in NS2A is located in the conserved hydrophobic residues of the predicted 2nd transmembrane region. It is possible that the Leu46 to polar His substitution affects the membrane spanning domain and the interaction with other transmembrane domains of NS2A or other membrane-associated viral proteins. A change in membrane associated protein topology could lead to a defect in the replication properties of NS2A such as the formation of the replication complex by binding with viral RNA and other components of the replication complex.

NS5 is the largest (104 kDa) of the flavivirus proteins, and three functional domains have been identified in NS5: a *S*-adenosylmethionine methyltransferase-like domain in the N-terminal region (Egloff et al., 2002; Koonin, 1993; Ray et al., 2006), a centrally located nuclear localization sequence (NLS) (Forwood et al., 1999; Kapoor et al., 1995), and an RNA-dependent RNA polymerase (RdRp) domain in the C-terminal region (Bartholomeusz and Wright, 1993; Koonin, 1991). The Asp836 residue in NS5 is located in the RdRp domain. In the homology model of OHFV RdRp domain based on the crystal structure of the dengue virus RdRp domain, this residue is within the α25 helix in the Thumb domain (Yap et al., 2007). In position 836 of the NS5 RdRp domain, negatively charged amino acids aspartic acid or glutamic acid are highly conserved among most flaviviruses. The molecular model suggests that the negatively charged Asp836 might form a salt bridge with the positively charged Lys720 in Motif E of the RdRp domain (Fig. 7). Molecular mechanics calculations also showed that the Asp836 to Gly substitution significantly reduced the interaction of the residue at position 836 with the Lys720 and Motif E (supplementary Table 1). These results led to the hypothesis that the reduction of interaction due to Asp836 to Gly substitution causes structural fluctuation, especially in Motif E. Motif E forms an antiparallel β-sheet wedged between the palm domain and several α-helices of the thumb domain. In several studies, it has been shown that some of the residues in Motif E are involved in the GTP-binding site and which have essential roles in *de novo* initiation of RNA synthesis in *Flaviviridae* polymerases (Choi et al., 2004; Lai et al., 1999; Yap et al.,

2007). It is possible that residue Asp836 is important for the structural stability of Motif E, and that the structural fluctuation of Motif E caused by the Asp836 to Gly substitution leads to a reduction in the efficiency of *de novo* initiation of RNA synthesis. In general, the conformational fluctuation of proteins is associated with their temperature. Therefore, this thermal fluctuation could be a possible cause of the temperature-sensitive property observed in the replicon studies (Fig. 5). Temperature dependence has been reported at the initiation, but not elongation, phase of *de novo* RNA synthesis by dengue virus RdRp (Ackermann and Padmanabhan, 2001). These data support the involvement of the interaction between Asp836 and Motif E in *de novo* initiation of RNA synthesis.

In summary, we have constructed an infectious cDNA clone of OHFV and demonstrated the utility of this clone in the research of OHFV pathogenesis. We have also identified previously unknown mutations in NS2A and NS5 that appear to play important roles in OHFV RNA synthesis.

Acknowledgments

This work was supported by Overseas Assignment Program for Japanese Researchers in Research into Emerging and Re-emerging Infectious Diseases from The Japan Health Sciences Foundation and Grants-in-Aid for Scientific Research from the Ministry of Education, Science, Sports, and Culture of Japan, Health Sciences Grants for Research on Emerging and Re-emerging Infectious Disease from the Ministry of Health, Labour, and Welfare of Japan, and a Western Regional Center of Excellence (U54 AI057156) Career Development award (MRH) in part.

Appendix A. Supplementary data

Supplementary data associated with this article can be found, in the online version, at doi:10.1016/j.virusres.2010.08.023.

References

Ackermann, M., Padmanabhan, R., 2001. De novo synthesis of RNA by the dengue virus RNA-dependent RNA polymerase exhibits temperature dependence at the initiation but not elongation phase. J. Biol. Chem. 276 (43), 39926–39937.

Bartholomeusz, A.I., Wright, P.J., 1993. Synthesis of dengue virus RNA in vitro: initiation and the involvement of proteins NS3 and NS5. Arch. Virol. 128 (1–2), 111–121.

Bredenbeek, P.J., Kooi, E.A., Lindenbach, B., Huijkman, N., Rice, C.M., Spaan, W.J., 2003. A stable full-length yellow fever virus cDNA clone and the role of conserved RNA elements in flavivirus replication. J Gen Virol 84 (Pt 5), 1261–1268.

Buchen-Osmond, C., 2003. 00.026.0.01.046.02. Tick-borne encephalitis virus group. In: Buchen-Osmond, C. (Ed.), ICTVdB—The Universal Virus Database, Version 3. ICTVdB Management, Columbia University, New York, USA.

Burke, D.S., Monath, T.P., 2001. Flaviviruses. In: Knipe, D.M., Howley, P.M. (Eds.), Fields' Virology, 4th ed. Lippincott Williams & Wilkins, Philadelphia, pp. 1043–1125.

Busygin, F.F., 2000. Omsk hemorrhagic fever—current status of the problem. Vopr. Virusol. 45 (3), 4–9.

Campbell, M.S., Pletnev, A.G., 2000. Infectious cDNA clones of Langat tick-borne flavivirus that differ from their parent in peripheral neurovirulence. Virology 269 (1), 225–237.

Chambers, T.J., Hahn, C.S., Galler, R., Rice, C.M., 1990. Flavivirus genome organization, expression, and replication. Annu. Rev. Microbiol. 44, 649–688.

Choi, K.H., Groarke, J.M., Young, D.C., Kuhn, R.J., Smith, J.L., Pevear, D.C., Rossmann, M.G., 2004. The structure of the RNA-dependent RNA polymerase from bovine viral diarrhea virus establishes the role of GTP in de novo initiation. Proc. Natl. Acad. Sci. U.S.A. 101 (13), 4425–4430, The PyMol Molecular Graphics System. DeLano Scientific, San Carlos, CA.

DeLano, W.L., 2002. The PyMol Molecular Graphics System. DeLano Scientific, San Carlos, CA.

Egloff, M.P., Benarroch, D., Selisko, B., Romette, J.L., Canard, B., 2002. An RNA cap (nucleoside-2'-O-)-methyltransferase in the flavivirus RNA polymerase NS5: crystal structure and functional characterization. EMBO J. 21 (11), 2757–2768.

Eisenberg, D., Luthy, R., Bowie, J.U., 1997. VERIFY3D: assessment of protein models with three-dimensional profiles. Methods Enzymol. 277, 396–404.

Eswar, N., John, B., Mirkovic, N., Fiser, A., Ilyin, V.A., Pieper, U., Stuart, A.C., Marti-Renom, M.A., Madhusudhan, M.S., Yerkovich, B., Sali, A., 2003. Tools for comparative protein structure modeling and analysis. Nucleic Acids Res. 31 (13), 3375–3380.

Forwood, J.K., Brooks, A., Briggs, L.J., Xiao, C.Y., Jans, D.A., Vasudevan, S.G., 1999. The 37-amino-acid interdomain of dengue virus NS5 protein contains a functional NLS and inhibitory CK2 site. Biochem. Biophys. Res. Commun. 257 (3), 731–737.

Gritsun, T.S., Gould, E.A., 1998. Development and analysis of a tick-borne encephalitis virus infectious clone using a novel and rapid strategy. J. Virol. Methods 76 (1–2), 109–120.

Gritsun, T.S., Venugopal, K., Zanotto, P.M., Mikhailov, M.V., Sall, A.A., Holmes, E.C., Polkinghorne, I., Frolova, T.V., Pogodina, V.V., Lashkevich, V.A., Gould, E.A., 1997. Complete sequence of two tick-borne flaviviruses isolated from Siberia and the UK: analysis and significance of the 5′ and 3′-UTRs. Virus Res. 49 (1), 27–39.

Hayasaka, D., Gritsun, T.S., Yoshii, K., Ueki, T., Goto, A., Mizutani, T., Kariwa, H., Iwasaki, T., Gould, E.A., Takashima, I., 2004. Amino acid changes responsible for attenuation of virus neurovirulence in an infectious cDNA clone of the Oshima strain of tick-borne encephalitis virus. J. Gen. Virol. 85 (Pt 4), 1007–1018.

Hofmann, K., Stoffel, W., 1993. TMbase—a database of membrane spanning proteins segments. Biol. Chem. Hoppe-Seyler 374, 166.

Holbrook, M.R., Aronson, J.F., Campbell, G.A., Jones, S., Feldmann, H., Barrett, A.D., 2005. An animal model for the tickborne flavivirus—Omsk hemorrhagic fever virus. J. Infect. Dis. 191 (1), 100–108.

Kapoor, M., Zhang, L., Ramachandra, M., Kusukawa, J., Ebner, K.E., Padmanabhan, R., 1995. Association between NS3 and NS5 proteins of dengue virus type 2 in the putative RNA replicase is linked to differential phosphorylation of NS5. J. Biol. Chem. 270 (32), 19100–19106.

Kharitonova, N.N., Leonov, Y.A., 1985. Omsk Hemorrhagic Fever (S. Korzelska, Trans.) Amerind Publishing Co., New Delhi.

Kinney, R.M., Butrapet, S., Chang, G.J., Tsuchiya, K.R., Roehrig, J.T., Bhamarapravati, N., Gubler, D.J., 1997. Construction of infectious cDNA clones for dengue 2 virus: strain 16681 and its attenuated vaccine derivative, strain PDK-53. Virology 230 (2), 300–308.

Koonin, E.V., 1991. The phylogeny of RNA-dependent RNA polymerases of positive-strand RNA viruses. J. Gen. Virol. 72 (Pt 9), 2197–2206.

Koonin, E.V., 1993. Computer-assisted identification of a putative methyltransferase domain in NS5 protein of flaviviruses and lambda 2 protein of reovirus. J. Gen. Virol. 74 (Pt 4), 733–740.

Krogh, A., Larsson, B., von Heijne, G., Sonnhammer, E.L., 2001. Predicting transmembrane protein topology with a hidden Markov model: application to complete genomes. J. Mol. Biol. 305 (3), 567–580.

Kummerer, B.M., Rice, C.M., 2002. Mutations in the yellow fever virus nonstructural protein NS2A selectively block production of infectious particles. J. Virol. 76 (10), 4773–4784.

Lai, V.C., Kao, C.C., Ferrari, E., Park, J., Uss, A.S., Wright-Minogue, J., Hong, Z., Lau, J.Y., 1999. Mutational analysis of bovine viral diarrhea virus RNA-dependent RNA polymerase. J. Virol. 73 (12), 10129–10136.

Laskowski, R.A., Macarthur, M.W., Moss, D.S., Thornton, J.M., 1993. Procheck—a program to check the stereochemical quality of protein structures. J. Appl. Cryst. 26, 283–291.

Leung, J.Y., Pijlman, G.P., Kondratieva, N., Hyde, J., Mackenzie, J.M., Khromykh, A.A., 2008. Role of nonstructural protein NS2A in flavivirus assembly. J. Virol. 82 (10), 4731–4741.

Liu, W.J., Chen, H.B., Khromykh, A.A., 2003. Molecular and functional analyses of Kunjin virus infectious cDNA clones demonstrate the essential roles for NS2A in virus assembly and for a nonconservative residue in NS3 in RNA replication. J. Virol. 77 (14), 7804–7813.

Liu, W.J., Chen, H.B., Wang, X.J., Huang, H., Khromykh, A.A., 2004. Analysis of adaptive mutations in Kunjin virus replicon RNA reveals a novel role for the flavivirus nonstructural protein NS2A in inhibition of beta interferon promoter-driven transcription. J. Virol. 78 (22), 12225–12235.

Liu, W.J., Wang, X.J., Clark, D.C., Lobigs, M., Hall, R.A., Khromykh, A.A., 2006. A single amino acid substitution in the West Nile virus nonstructural protein NS2A disables its ability to inhibit alpha/beta interferon induction and attenuates virus virulence in mice. J. Virol. 80 (5), 2396–2404.

Liu, W.J., Wang, X.J., Mokhonov, V.V., Shi, P.Y., Randall, R., Khromykh, A.A., 2005. Inhibition of interferon signaling by the New York 99 strain and Kunjin subtype of West Nile virus involves blockage of STAT1 and STAT2 activation by nonstructural proteins. J. Virol. 79 (3), 1934–1942.

Mackenzie, J.M., Khromykh, A.A., Jones, M.K., Westaway, E.G., 1998. Subcellular localization and some biochemical properties of the flavivirus Kunjin nonstructural proteins NS2A and NS4A. Virology 245 (2), 203–215.

Mandl, C.W., Ecker, M., Holzmann, H., Kunz, C., Heinz, F.X., 1997. Infectious cDNA clones of tick-borne encephalitis virus European subtype prototypic strain Neudoerfl and high virulence strain Hypr. J. Gen. Virol. 78 (Pt 5), 1049–1057.

Mason, P.W., Bezborodova, S.V., Henry, T.M., 2002. Identification and characterization of a cis-acting replication element (cre) adjacent to the internal ribosome entry site of foot-and-mouth disease virus. J. Virol. 76 (19), 9686–9694.

McElroy, K.L., Tsetsarkin, K.A., Vanlandingham, D.L., Higgs, S., 2005. Characterization of an infectious clone of the wild-type yellow fever virus Asibi strain that is able to infect and disseminate in mosquitoes. J. Gen. Virol. 86 (Pt 6), 1747–1751.

Mendez, E., Ruggli, N., Collett, M.S., Rice, C.M., 1998. Infectious bovine viral diarrhea virus (strain NADL) RNA from stable cDNA clones: a cellular insert determines NS3 production and viral cytopathogenicity. J. Virol. 72 (6), 4737–4745.

Munoz-Jordan, J.L., Sanchez-Burgos, G.G., Laurent-Rolle, M., Garcia-Sastre, A., 2003. Inhibition of interferon signaling by dengue virus. Proc. Natl. Acad. Sci. U.S.A. 100 (24), 14333–14338.

Pletnev, A.G., 2001. Infectious cDNA clone of attenuated Langat tick-borne flavivirus (strain E5) and a 3′ deletion mutant constructed from it exhibit decreased neuroinvasiveness in immunodeficient mice. Virology 282 (2), 288–300.

Proutski, V., Gould, E.A., Holmes, E.C., 1997. Secondary structure of the 3′ untranslated region of flaviviruses: similarities and differences. Nucleic Acids Res. 25 (6), 1194–1202.

Rauscher, S., Flamm, C., Mandl, C.W., Heinz, F.X., Stadler, P.F., 1997. Secondary structure of the 3′-noncoding region of flavivirus genomes: comparative analysis of base pairing probabilities. Rna 3 (7), 779–791.

Ray, D., Shah, A., Tilgner, M., Guo, Y., Zhao, Y., Dong, H., Deas, T.S., Zhou, Y., Li, H., Shi, P.Y., 2006. West Nile virus 5′-cap structure is formed by sequential guanine N-7 and ribose 2′-O methylations by nonstructural protein 5. J. Virol. 80 (17), 8362–8370.

Rossi, S.L., Zhao, Q., O'Donnell, V.K., Mason, P.W., 2005. Adaptation of West Nile virus replicons to cells in culture and use of replicon-bearing cells to probe antiviral action. Virology 331 (2), 457–470.

Ruggli, N., Tratschin, J.D., Mittelholzer, C., Hofmann, M.A., 1996. Nucleotide sequence of classical swine fever virus strain Alfort/187 and transcription of infectious RNA from stably cloned full-length cDNA. J. Virol. 70 (6), 3478–3487.

Shi, P.Y., Tilgner, M., Lo, M.K., Kent, K.A., Bernard, K.A., 2002. Infectious cDNA clone of the epidemic west nile virus from New York City. J. Virol. 76 (12), 5847–5856.

Still, W.C., Tempczyk, A., Hawley, R.C., Hendrickson, T., 1990. Semianalytical treatment of solvation for molecular mechanics and dynamics. J. Am. Chem. Soc. 112 (16), 6127–6129.

Tigabu, B., Juelich, T., Bertrand, J., Holbrook, M.R., 2009. Clinical evaluation of highly pathogenic tick-borne flavivirus infection in the mouse model. J. Med. Virol. 81 (7), 1261–1269.

Tsui, V., Case, D.A., 2000. Theory and applications of the generalized Born solvation model in macromolecular simulations. Biopolymers 56 (4), 275–291.

Yamshchikov, V., Mishin, V., Cominelli, F., 2001. A new strategy in design of +RNA virus infectious clones enabling their stable propagation in E. coli. Virology 281 (2), 272–280.

Yap, T.L., Xu, T., Chen, Y.L., Malet, H., Egloff, M.P., Canard, B., Vasudevan, S.G., Lescar, J., 2007. Crystal structure of the dengue virus RNA-dependent RNA polymerase catalytic domain at 1.85-angstrom resolution. J. Virol. 81 (9), 4753–4765.

Yoshii, K., Hayasaka, D., Goto, A., Kawakami, K., Kariwa, H., Takashima, I., 2005. Packaging the replicon RNA of the Far-Eastern subtype of tick-borne encephalitis virus into single-round infectious particles: development of a heterologous gene delivery system. Vaccine 23 (30), 3946–3956.

Yoshii, K., Holbrook, M.R., 2009. Sub-genomic replicon and virus-like particles of Omsk hemorrhagic fever virus. Arch. Virol. 154 (4), 573–580.

Yoshii, K., Konno, A., Goto, A., Nio, J., Obara, M., Ueki, T., Hayasaka, D., Mizutani, T., Kariwa, H., Takashima, I., 2004. Single point mutation in tick-borne encephalitis virus prM protein induces a reduction of virus particle secretion. J. Gen. Virol. 85 (Pt 10), 3049–3058.

Yun, S.I., Kim, S.Y., Rice, C.M., Lee, Y.M., 2003. Development and application of a reverse genetics system for Japanese encephalitis virus. J. Virol. 77 (11), 6450–6465.